processes

MDPI

Article

Self-Sustaining Control Strategy for Proton-Exchange Membrane Electrolysis Devices Based on Gradient-Disturbance Observation Method

Zihang Gao and Yizhi Tian *

College of Electrical Engineering, Xinjiang University, Urumqi 830017, China
* Correspondence: ttarsenal@xju.edu.cn

Abstract: This paper proposes a self-sustaining control model for proton-exchange membrane (PEM) electrolysis devices, aiming to maintain the temperature of their internal operating environment and, thus, improve the electrolysis efficiency and hydrogen production rate. Based on the analysis of energy–substance balance and electrochemical reaction characteristics, an electrothermal-coupling dynamic model for PEM electrolysis devices was constructed. Considering the influence of the input energy–substance and the output hydrogen and oxygen of PEM electrolysis devices on the whole dynamic equilibrium process, the required electrical energy and water molar flow rate are dynamically adjusted so that the temperature of the cathode and the anode is maintained near 338.15 K. The analytical results show that the hydrogen production rate and electrolysis efficiency are increased by 0.275 mol/min and 3.9%, respectively, by linearly stacking 100 PEM electrolysis devices to form a hydrogen production system with constant cathode and anode operating temperatures around 338.15 K in the self-sustaining controlled mode.

Keywords: proton-exchange membrane electrolysis device; self-sustaining control; electrothermal-coupling dynamic model; gradient method; disturbance observation method

Citation: Gao, Z.; Tian, Y. Self-Sustaining Control Strategy for Proton-Exchange Membrane Electrolysis Devices Based on Gradient-Disturbance Observation Method. *Processes* **2023**, *11*, 828. https://doi.org/10.3390/pr11030828

Academic Editors: Jiangxin Wang and Gang Wang

Received: 2 January 2023
Revised: 7 March 2023
Accepted: 8 March 2023
Published: 10 March 2023

1. Introduction

Hydrogen energy has a high energy density and is pollution-free, making it an excellent alternative to fossil fuels [1]. It has become a key part of the strategies aiming at limiting carbon dioxide emissions and achieving global decarbonization. Compared to alkaline electrolysis technology, proton-exchange membrane (PEM) electrolysis technology has the advantages of high current density, low energy consumption, high hydrogen production pressure, and rapid dynamic adjustment [2]. However, temperature has a significant impact on the safe and efficient operation of PEM electrolysis devices within a wide power range, and it is necessary to establish a comprehensive dynamic mathematical model during the physical and chemical transformation processes. By controlling the operating temperature of both the anode and cathode, the hydrogen production rate and electrolysis efficiency can be improved.

Currently, the electrolysis efficiency of PEM electrolysis devices is mainly defined by voltage conversion and energy conversion. In the study of reference [3], the electrolysis efficiency of PEM electrolysis devices is defined as the ratio of the minimum theoretical voltage required for electrolysis to the input voltage. In the study of reference [4], the electrolysis efficiency of PEM electrolysis devices is defined as the ratio of the thermoneutral voltage that does not produce excess heat during the exothermic reaction of electrolyzing water to the input voltage. In the study of reference [5], the electrolysis efficiency of PEM electrolysis devices is defined as the ratio of the high heating value (HHV) voltage derived from the influence of temperature and pressure on the enthalpy of the water electrolysis reaction to the input voltage. In the studies of references [6,7], the electrolysis efficiency of PEM electrolysis devices is defined as the ratio of the produced HHV and low heating value

(LHV) of hydrogen gas to the input electrical energy. Considering various losses during the operation of PEM electrolysis devices, the study of reference [8] defines electrolysis efficiency as the ratio of the electrical energy consumed in the electrolysis reaction under ideal and actual states. None of these studies have considered the energy consumption of an external water circulation device during the work process.

The thermal model of a PEM electrolysis device is the basis for temperature control. Currently, PEM electrolysis devices' lumped heat capacity model is mainly used as their thermal model. Studies [9,10] have shown that the lumped heat capacity model of PEM electrolysis devices is constructed as a thermal model by combining an equivalent circuit model and a mass transport model, but this model treats the anode and the cathode as a whole, thereby ignoring the temperature difference between the two. A study [11] has shown that a lumped heat capacity model is constructed as a thermal model by considering the heat provided by an external circulating water heating device and the heat taken away by the cooling fan, but it ignores the heat generated by the current passing through the anode and cathode. Another study [12] has shown that while gradually increasing the current density of a PEM electrolysis device, a linear thermal model of the operating power and temperature is constructed through the least squares method by measuring its temperature using the temperature sensors and thermal imaging cameras located on its surface, but this model ignores the sudden change in temperature caused by the sudden mutation of current density. Several studies [13,14] have shown that by analyzing the heat generated, lost, and taken away by the cooling device of a PEM electrolysis device, a lumped heat capacity model is constructed as a thermal model, but it ignores the heat taken away by the products.

PEM electrolysis devices are sensitive to temperature changes, and operating at too low or too high temperatures can negatively affect their efficiency and longevity. Therefore, it is important to control the operating temperature of PEM electrolysis devices to ensure their safe, efficient, and sustainable operation. Several studies have explored the impact of temperature on PEM electrolysis devices. One study [15] found that during the start-up phase of a grid-connected PEM electrolysis device, coordinating the power of the heating system with the start-up power of the PEM electrolysis device can raise the operating temperature and improve the electrolysis efficiency. Another study [16] investigated an integrated system consisting of a photovoltaic cell and a PEM electrolysis device and found that pre-heating the water required for electrolysis by absorbing a portion of the heat from the photovoltaic cell and controlling the speed at which it enters the PEM electrolysis device can also improve the efficiency. Another study [17] investigated the impact of temperature on the electrolysis efficiency of PEM electrolysis devices during the entire operating phase and found that maintaining an operating temperature of 60 °C can yield higher efficiency compared to when operating at 20 °C. Additionally, a few studies [18,19] found that operating at higher temperatures within the range of 313.15–353.15 K can effectively reduce the operating voltage of PEM electrolysis devices and improve efficiency. However, it is important to note that operating at excessively high temperatures can also damage the structure of PEM and shorten the lifespan of PEM electrolysis devices, as demonstrated by a previous study [20]. Therefore, a balance between efficiency and safety must be maintained when controlling the operating temperature of PEM electrolysis devices.

Currently, based on the equivalent circuit modeling of PEM electrolysis devices, these models can be classified into steady-state and dynamic models depending on the operating conditions. Research studies [21,22] have shown that a steady-state model can be constructed by fitting the voltage–current characteristic curve of a PEM electrolysis device under constant temperature and pressure conditions, considering the voltage threshold at the beginning of the current stage, and building the model in the form of a series connection of counter electromotive force and resistance. A previous research study [23] has shown that the voltage of an electrolysis device is composed of reversible voltage and overvoltage that characterize three electrolysis reactions, which can be combined to construct a static equivalent circuit model in the form of a series connection of four counter electromotive

forces. Another research study [24] has shown that a dynamic equivalent circuit model can be constructed by fitting the current–voltage relationship curve using the least squares regression algorithm based on the voltage response of a PEM electrolysis device under different input currents. The model is in the form of a series connection of a counter electromotive force, a resistance, and two parallel resistance–capacitance combinations, with all parameters in the circuit being treated as constants. Other research studies [25,26] have shown that, based on a static equivalent circuit model of PEM electrolysis devices, the parameters of the model cannot be regarded as constants due to the changes in the input current. By testing the voltage response under different input currents, a dynamic equivalent circuit model in the form of a series connection of a counter electromotive force, a resistance, and two parallel resistance–capacitance combinations can be constructed, where the two parallel resistance–capacitance parameters are the functions of the input current. This model is suitable for operating conditions with dynamic changes in the input current but does not consider the influence of temperature on the model parameters.

Under the premise of external power variation, a PEM device self-sustaining control strategy based on the gradient-disturbance observation method is proposed to maintain the operating temperature of the anode and cathode for high electrolysis efficiency. A dynamic equivalent circuit based on electrothermal-coupling, including the threshold voltage phenomenon, the cathode and anode activation phenomenon, and the energy loss phenomenon, is constructed. It controls the input voltage of the cathode and anode and the molar flow rate of the water outlet, does not require external cooling devices, keeps the operating temperature of the cathode and anode constant near the set value, and can improve the hydrogen production rate and electrolysis efficiency. Based on the construction of an electrothermal-coupling dynamic equivalent circuit of a single electrolysis device, the analysis of the self-sustaining control strategy is carried out by linearly stacking multiple electrolysis devices to form a hydrogen production system.

2. PEM Electrolysis Device's Basic Structure and Dynamic Equivalent Circuit Model

2.1. PEM Electrolysis Device's Basic Structure

With the proton-exchange membrane as the center, the catalyst layer, gas diffusion layer, and electrode plate of the anode and cathode are closely connected on both sides in turn and symmetrically form the main part of a PEM electrolysis device. The specific structure is shown in Figure 1.

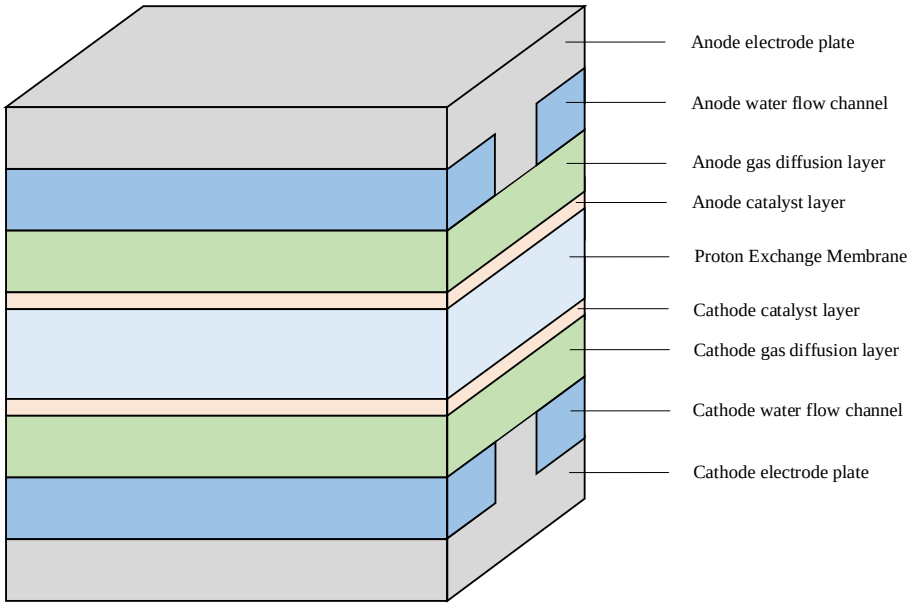

Figure 1. The specific structure of the PEM electrolysis device.

It is well known that several voltage drops occur when the input voltage is applied to a PEM electrolysis device, namely the reversible voltage, the activation overvoltage, the diffusion overvoltage, and the ohmic overvoltage [26]. Among them, the diffusion overvoltage is two orders of magnitude smaller than the other overvoltages, so this voltage is often neglected. These voltage drops are nonlinearly related to the current [27], and according to Kirchhoff's voltage law, their voltage representation is specified as follows:

$$U_{cell} = U_{rev} + U_{act,cat} + U_{act,an} + U_{ohm} \quad (1)$$

The specific variables in the formula are shown in Table 1.

Table 1. Variables of the operating voltage formula.

	Symbol	Name	Unit
Variables	U_{cell}	Operating voltage	V
	U_{rev}	Reversible voltage	V
	$U_{act,cat}$	Cathode activation overvoltage	V
	$U_{act,an}$	Anode activation overvoltage	V
	U_{ohm}	Ohmic overvoltage	V

Among them, the reversible voltage, the cathode and anode activation overvoltage, and the ohmic overvoltage correspond to three chemical phenomena in the electrolysis process: the threshold voltage phenomenon, the cathode and anode activation phenomenon, and the energy loss phenomenon, respectively.

2.2. Threshold Voltage Phenomenon in the Electrolysis Process

The phenomenon that the input voltage to a PEM electrolysis device gradually increases to a certain value before the operating current occurs is called the threshold voltage phenomenon. This voltage is the minimum voltage required for the decomposition of water into hydrogen and oxygen bodies and is called the reversible voltage, which can be expressed by the Nernst equation [19] as follows:

$$U_{rev} = 1.229 - 0.9 \times 10^{-3}(T_{cell} - 298.15) + \frac{RT_{cell}}{2F} \ln\left(\frac{p_{H_2} p_{O_2}^{\frac{1}{2}}}{a_{H_2O}}\right) \quad (2)$$

The specific parameters and variables in the formula are shown in Table 2.

Table 2. Parameters and variables of the reversible voltage formula.

	Symbol	Name	Unit
Parameters	R	Universal gas constant	J/(mol·K)
	F	Faraday constant	C/mol
	a_{H_2O}	Water activity in the anode	-
Variables	T_{cell}	Operating temperature	K
	p_{H_2}	Hydrogen pressure in the cathode	Pa
	p_{O_2}	Oxygen pressure in the anode	Pa

2.3. Activation Phenomenon of Cathode and Anode in the Electrolysis Process

The activation phenomenon is the transfer or exchange of charged particles between the electrode and the electrolyte during the dynamic hydrogen production process in a PEM electrolysis device, and two layers of charges of opposite signs are formed on both sides of the partition interface, which is a phenomenon influenced by physical and chemical

factors, such as operating temperature, catalyst properties, and electrode morphology. The activation overvoltage is the occurrence of some irreversible loss of energy during the conversion process, which acts to drive electrons to or from the electrode during the chemical reaction, and which can be expressed by the Butler–Wolmer equation [28] as follows:

$$\begin{cases} U_{act,cat} = \frac{RT_{cat}}{\alpha_{cat}F}\sinh^{-1}\left[\frac{J}{2J_{0,cat}}\right] \\ U_{act,an} = \frac{RT_{an}}{\alpha_{an}F}\sinh^{-1}\left[\frac{J}{2J_{0,an}}\right] \end{cases} \quad (3)$$

The specific parameters and variables in the formula are shown in Table 3.

Table 3. Activation overvoltage formula's parameters and variables.

	Symbol	Name	Unit
Parameters	α_{cat}	Typical values for the charge transfer coefficient at the cathode	-
	α_{an}	Typical values for the charge transfer coefficient at the anode	-
	$J_{0,cat}$	Exchange current density on the cathode electrode	A/cm^2
	$J_{0,an}$	Exchange current density on the anode electrode	A/cm^2
Variables	T_{cat}	Operating temperature of the cathode	K
	T_{an}	Operating temperature of the anode	K
	J	Current density on the electrode	A/cm^2

In this process, a large number of charged particles exist at the interface between the electrode and the electrolyte, and the change in the degree of transfer or exchange of charged particles causes a change in the activation overvoltage of the cathode and the anode, which is accompanied by the formation of a double layer of charges of opposite signs and energy loss on both sides of the interface between the electrode and the electrolyte; this phenomenon and the dynamic process can be described by a resistive-capacitance parallel circuit [29].

The equivalent resistances, R_{cat} and R_{an}, which reflect the energy loss of this process, are determined as follows [25]:

$$\begin{cases} R_{cat} = \frac{U_{act,cat}}{I_{cell}} \\ R_{an} = \frac{U_{act,an}}{I_{cell}} \end{cases} \quad (4)$$

The specific variables in the formula are shown in Table 4.

Table 4. Variables of the equivalent resistance formula.

	Symbol	Name	Unit
Variables	R_{cat}	Equivalent resistance of the cathode	Ω
	R_{an}	Equivalent resistance of the anode	Ω
	I_{cell}	Operating current	A

The equivalent time constants, τ_{cat} and τ_{an}, can be used to represent the transition process in which the cathode and anode activation overvoltages reach stability when the excitation current changes, where the equivalent time constant τ_{cat} could be estimated as a current function; the proportional relationship exists between τ_{cat} and τ_{an} can be expressed as follows [25]:

$$\begin{cases} \tau_{cat} = 1.1562 \times \exp\left[\frac{-(I_{cell}-4.2672)^2}{0.09487}\right] + 0.606 \\ \tau_{an} = 0.1 \times \tau_{cat} \end{cases} \quad (5)$$

The specific variables in the formula are shown in Table 5.

Table 5. Variables of the equivalent time constant formula.

	Symbol	Name	Unit
Variables	τ_{cat}	Equivalent time constant of the cathode	s
	τ_{an}	Equivalent time constant of the anode	s

The equivalent capacitances, C_{cat} and C_{an}, in a resistive-capacitance parallel circuit based on the relationship between the equivalent time constants, τ_{cat} and τ_{an}, and the equivalent resistances, R_{cat} and R_{an}, are determined as follows [26]:

$$\begin{cases} \tau_{cat} = C_{cat} \times R_{cat} = C_{cat} \times \left(\frac{U_{act,cat}}{I_{cell}}\right) \\ \tau_{an} = C_{an} \times R_{an} = C_{an} \times \left(\frac{U_{act,an}}{I_{cell}}\right) \end{cases} \tag{6}$$

The specific variables in the formula are shown in Table 6.

Table 6. Variables of the equivalent capacitance formula.

	Symbol	Name	Unit
Variables	C_{cat}	Equivalent capacitance of the cathode	F
	C_{an}	Equivalent capacitance of the anode	F

2.4. Energy Loss Phenomenon in the Electrolysis Process

When a charge passes through the electrode plates and the gas diffusion layers of the cathode and anode, as well as the proton-exchange membrane, part of the electrical energy will be converted into heat energy and dissipated in the water; this phenomenon can be expressed by an equivalent resistance as follows:

$$\begin{cases} U_{ohm} = R_{ohm} \times I_{cell} \\ R_{ohm} = R_{mem} + R_{pl} + R_{el} \end{cases} \tag{7}$$

The specific parameters and variables in the formula are shown in Table 7.

Table 7. Parameters and variables of the ohmic overvoltage formula.

	Symbol	Name	Unit
Parameters	R_{pl}	Resistance of cathode and anode electrodes	Ω
	R_{el}	Resistance of cathode and anode gas diffusion layers	Ω
Variables	R_{mem}	Resistance of proton-exchange membrane	Ω
	R_{ohm}	PEM electrolysis device internal resistance	Ω

In summary, the dynamic equivalent circuit of a PEM electrolysis device can be represented as a voltage source, a counter electromotive force, resistance, and two resistive-capacitance structures in series, as shown in Figure 2.

The dynamic adjustment of the operating power can be achieved by adjusting the PEM electrolysis device's port voltage, which then changes the operating current and affects the changes in the above three phenomena. From the perspective of energy conversion, the complex coupling characteristics between electrical, chemical, and internal energy will affect the efficiency and the rate of the electrolysis process.

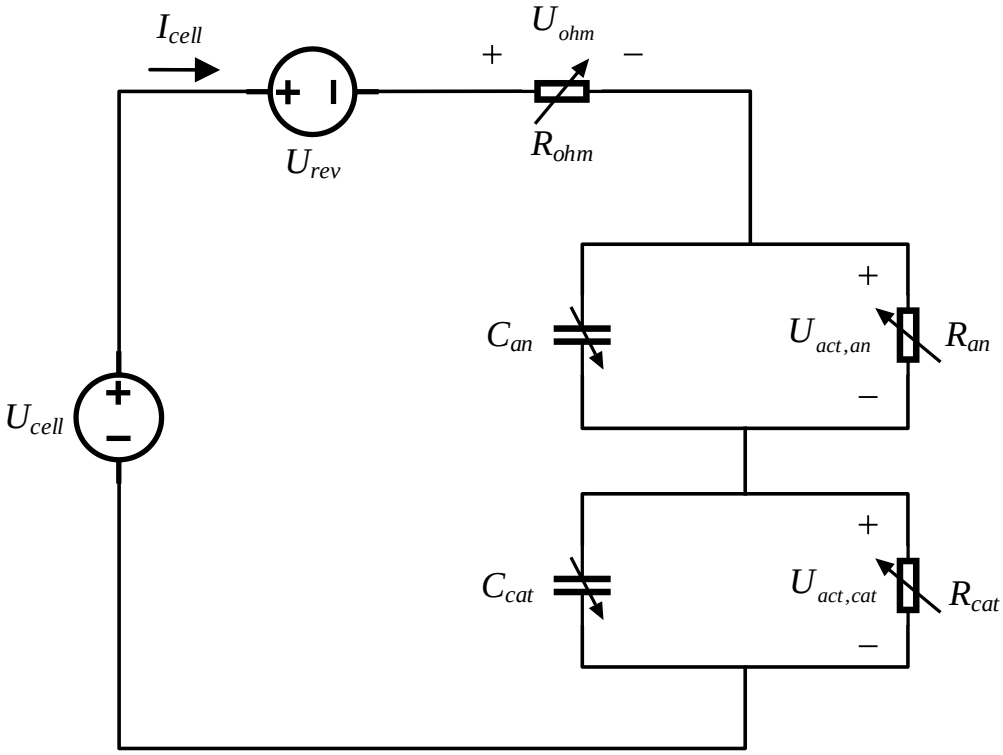

Figure 2. Dynamic equivalent circuit of a PEM electrolysis device.

3. Electrothermal-Coupling Dynamic Model of PEM Electrolysis Device

3.1. Analysis of Electrothermal Coupling Characteristics Inside PEM Electrolysis Device

When the external input power of the PEM electrolysis device and the internal gas molar flow rates and water molar flow rates change, the internal operating state is changed. The essence mentioned above is a complex energy transformation process between the electrical and chemical energy and the internal energy, as reflected in the interaction and restriction between electrolysis rate and operating temperature. Considering the comprehensive influence of the external input power, water flow, and output gas on heat, the internal temperature of the PEM electrolysis device will change and will then affect the electrolysis efficiency, as shown in Figure 3.

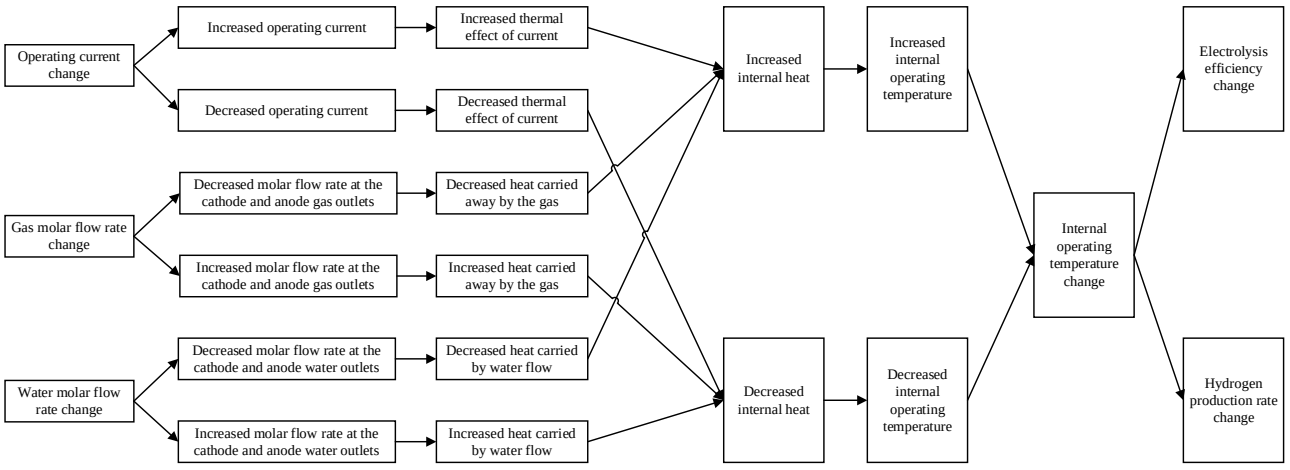

Figure 3. The effect of the combined changes in operating voltage, gas, and water flow rate on operating temperature.

3.2. Effect of Independent Change in Operating Voltage on Heat Generation in the Electrolysis Process

The energy–substance conversion process of electrolytic water is essentially a continuous chemical reaction in which the applied electrical energy stimulates the decomposition of a substance to absorb heat and is not spontaneous under certain conditions. When the input voltage exceeds the thermo-neutral voltage, the heat generated by the internal charge flowing through the resistance is absorbed by the circulating water flow.

The effect of an independent change in operating voltage on heat generation in the electrolysis process is as follows:

$$\begin{cases} \frac{dQ_{cat,1}}{dt} = \frac{1}{2}(U_{cell} - U_{th}) \times I_{cell} \\ \frac{dQ_{an,1}}{dt} = \frac{1}{2}(U_{cell} - U_{th}) \times I_{cell} \end{cases} \quad (8)$$

The specific parameters and variables in the formula are shown in Table 8.

Table 8. Parameters and variables of the heat formula for independent change in operating voltage.

	Symbol	Name	Unit
Parameters	U_{th}	Thermo-neutral voltage	V
Variables	$Q_{cat,1}$	Cathode heat when operating voltage varies independently	J
	$Q_{an,1}$	Anode heat when operating voltage varies independently	J

Since the PEM electrolysis device is connected to an external DC power supply, when the input power changes, the current thermal effect generated by the charge flowing through the dynamic equivalent circuit resistance responds in seconds, causing a faster variation in heat.

3.3. Effects of Independent Changes in Gas Molar Flow Rates and Water Molar Flow Rates on Heat Loss in the Electrolysis Process

There are two major factors affecting heat loss inside the PEM electrolysis device: gas molar flow rates and water molar flow rates.

The molar flow rates of water decomposition to produce hydrogen, oxygen, and water consumption, which is related to the operating current and Faraday efficiency, can be calculated using Faraday's law as follows [13]:

$$\begin{cases} F_{H_2,gen} = \frac{I_{cell}}{2F}\eta_F \\ F_{O_2,gen} = \frac{I_{cell}}{4F}\eta_F \\ F_{H_2O,con} = 1.25\frac{I_{cell}}{2F}\eta_F \end{cases} \quad (9)$$

The specific variables of the formula are shown in Table 9.

Table 9. Formula variables for molar flow rates of water decomposition to produce hydrogen, oxygen, and water consumption.

	Symbol	Name	Unit
Variables	$F_{H_2,gen}$	Molar flow rate of hydrogen generation at the cathode	mol/s
	$F_{O_2,gen}$	Molar flow rate of oxygen generation at the anode	mol/s
	$F_{H_2O,con}$	Molar flow rate of water consumed at the anode	mol/s
	η_F	Faraday efficiency	-

During the electrolysis process, based on the principle of electro-osmosis and the differences in water concentration and gas pressure between the cathode and anode, the

net molar flow rate of water being transferred from the anode to the cathode through the proton-exchange membrane is determined as follows [30]:

$$F_{H_2O,mem} = F_{H_2O,eod} + F_{H_2O,diff} - F_{H_2O,pe} \tag{10}$$

The specific variables of the formula are shown in Table 10.

Table 10. Net water molar flow formula's variables.

	Symbol	Name	Unit
Variables	$F_{H_2O,mem}$	Net molar flow rate of water through the proton-exchange membrane	mol/s
	$F_{H_2O,eod}$	Molar flow rate of water from the anode to the cathode due to electro-osmotic	mol/s
	$F_{H_2O,diff}$	Molar flow rate of water due to diffusion from the anode to the cathode	mol/s
	$F_{H_2O,pe}$	Molar flow rate of water from the cathode to the anode due to the pressure effect	mol/s

The effects of the independent changes in the molar rates of gas and water on heat loss during the electrolysis process are determined as follows:

$$\begin{cases} \frac{dQ_{cat,2}}{dt} = F^{cat}_{H_2O,out} \times C_{H_2O,v,m} \times (T_{cat} - T_1) + F_{H_2,out} \times C_{H_2,v,m} \times (T_{cat} - T_1) - F_{H_2O,mem} \times C_{H_2O,v,m} \times (T_{an} - T_{cat}) \\ \frac{dQ_{an,2}}{dt} = \left[\left(F^{an}_{H_2O,out} + F_{H_2O,mem} + F_{H_2O,con} \right) \times C_{H_2O,v,m} + F_{O_2,out} \times C_{O_2,v,m} \right] \times (T_{an} - T_1) \end{cases} \tag{11}$$

The specific parameters and variables in the formula are shown in Table 11.

Table 11. Parameters and variables of the heat formula for the independent variation in the molar flow rates of gas and water.

	Symbol	Name	Unit
Parameters	T_1	Environmental temperature	K
	$C_{H_2O,v,m}$	Constant capacity for the molar-specific heat capacity of water	J/(mol·K)
Variables	$Q_{cat,2}$	Cathode heat due to independent changes in molar flow rates of gas and water	J
	$Q_{an,2}$	Anode heat due to independent changes in molar flow rates of gas and water	J
	$F^{cat}_{H_2O,out}$	Molar flow rate of the water outlet in the cathode	mol/s
	$F_{H_2,out}$	Molar flow rate of the hydrogen outlet in the cathode	mol/s
	$F^{an}_{H_2O,out}$	Molar flow rate of the water outlet in the anode	mol/s
	$F_{O_2,out}$	Molar flow rate of the oxygen outlet in the anode	mol/s
	$C_{H_2,v,m}$	Constant capacity for the molar-specific heat capacity of hydrogen	J/(mol·K)
	$C_{O_2,v,m}$	Constant capacity for the molar-specific heat capacity of oxygen	J/(mol·K)

In the electrolysis process, the molar flow rates of water consumption and transmission from the anode to the cathode through the proton-exchange membrane are minute, while the molar flow rates of gas and water outlets at the anode and cathode are relatively large. However, a comprehensive analysis shows that the molar flow rates of gas and water are slower than the operating voltage, resulting in sluggish heat change.

3.4. Effects of Combined Changes in Operating Voltage and Molar Flow Rates of Gas and Water on Heat Loss in the Electrolysis Process

According to the superposition principle, heat variations in the cathode and anode under the two operating conditions mentioned above are superimposed. The combined

changes in operating voltage and molar flow rates of gas and water in the electrolysis process affect the heat are as follows:

$$\begin{cases} \frac{dQ_{cat}}{dt} = \frac{dQ_{cat,1} - dQ_{cat,2}}{dt} \\ \frac{dQ_{an}}{dt} = \frac{dQ_{an,1} - dQ_{an,2}}{dt} \end{cases} \quad (12)$$

The specific variables in the formula are shown in Table 12.

Table 12. Variables of the heat formula for combined changes in operating voltage and molar flow rates of gas and water.

	Symbol	Name	Unit
Variables	Q_{cat}	Cathode heat due to combined changes in operating voltage and molar flow rates of gas and water	J
	Q_{an}	Anode heat due to combined changes in operating voltage and molar flow rates of gas and water	J

3.5. Effect of Heat Change on Operating Temperature

According to the specific heat capacity formula, the operating temperatures of the cathode and the anode are determined as follows:

$$\begin{cases} \frac{dT_{cat}}{dt} = \frac{\frac{dQ_{cat}}{dt}}{0.5C_t} \\ \frac{dT_{an}}{dt} = \frac{\frac{dQ_{an}}{dt}}{0.5C_t} \end{cases} \quad (13)$$

The specific parameters in the formula are shown in Table 13.

Table 13. Parameters of the operating temperature formula.

	Symbol	Name	Unit
Variables	C_t	PEM electrolysis device's thermal capacity	J/K

The operating current, gas molar flow rates, and water molar flow rates all affect the balance of internal heat generation and loss, causing a wide range of operating temperature changes, which affects the electrolysis rate and efficiency. The above three are coupled and constrained by each other; therefore, it is necessary to build appropriate control strategies to improve the electrolysis rate and efficiency.

4. PEM Electrolysis Device Self-Sustaining Control Strategy

4.1. PEM Electrolysis Device Self-Sustaining Control Definition

By controlling the input and output energy–substance of the PEM electrolysis device in real time, the operating temperature is dynamically adjusted to keep the efficiency at a high level by using the heat generated and lost during the operation of the PEM electrolysis device, which is defined as "self-sustaining control" in this paper. Specifically, the molar flow rates of the cathode and anode gas and water outlets inside the PEM electrolysis device and the electrical power input from the external DC power supply are adjusted to maintain constant operating temperatures at the cathode and anode. The Faraday efficiency and electrolysis efficiency are optimal when the internal gas pressure is at atmospheric pressure [31,32], and at this time, the molar flow rate of the internal cathode and anode gas outlets is equal to the molar flow rate of the produced gas. The whole control process is aimed at maintaining a constant operating temperature to match the power variation within the constraints of the electrolysis efficiency. This is shown in Figure 4.

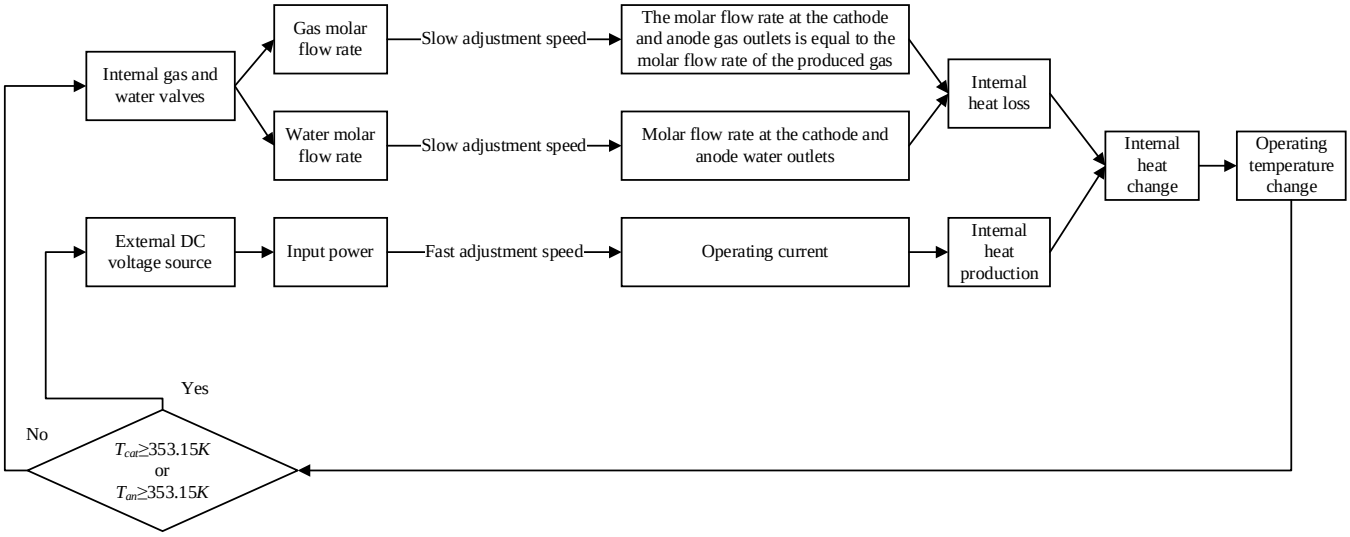

Figure 4. Self-sustaining control definition.

4.2. PEM Electrolysis Device's Electrolysis Efficiency Definition

Based on the high heating value of the hydrogen produced by the PEM electrolysis device, and the external water circulation device that provides water circulation, the electrolysis efficiency is redefined by looking at the overall energy system, as shown in Figure 5.

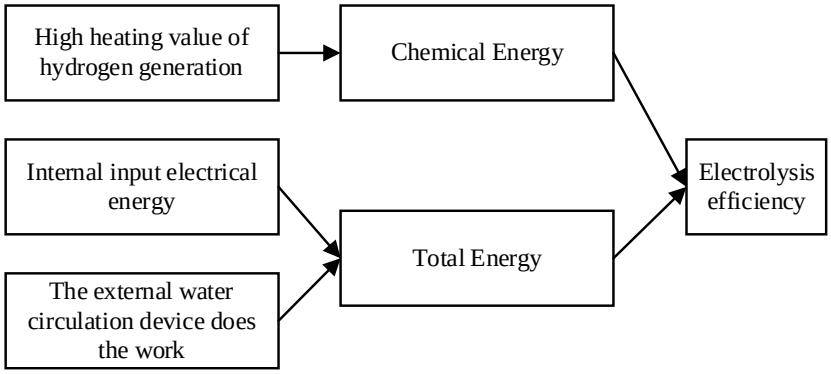

Figure 5. Definition of electrolysis efficiency.

Assuming the efficiency of the external water circulation device is 0.85, the work it performs is specified as follows:

$$W_w = \frac{\int_0^t \left(F_{H_2O,out}^{an} + F_{H_2O,con} + F_{H_2O,out}^{cat} \right) dt \times \frac{18 \times g \times h_w}{1000}}{0.85} \quad (14)$$

The specific parameters and variable in the formula are shown in Table 14.

Table 14. Parameters and variable of the formula for the external water circulation device's work.

	Symbol	Name	Unit
Parameters	g	Gravitational acceleration	m/s^2
	h_w	Water refill tank height	m
Variable	W_w	Work performed by the external water circulation device	J

The high heating value of the generated hydrogen is specified as follows:

$$W_{H_2} = \int_0^t F_{H_2,gen} dt \times Q_{H_2,HHV} \tag{15}$$

The specific parameter in the formula is shown in Table 15.

Table 15. Parameter of the high heating value formula for the production of hydrogen.

	Symbol	Name	Unit
Parameter	$Q_{H_2,HHV}$	High heating value per mole of hydrogen	J/mol

Then, the electrolysis efficiency of the PEM electrolysis device is defined as follows:

$$\eta_{cell} = \frac{W_{H_2}}{\int_0^t U_{cell} I_{cell} dt + W_w} \tag{16}$$

The specific variable in the formula is shown in Table 16.

Table 16. Variable of the electrolysis efficiency definition formula.

	Symbol	Name	Unit
Variable	η_{cell}	Electrolysis efficiency	-

4.3. PEM Electrolysis Device's Energy Consumption Ratio Definition

The cost-effectiveness of hydrogen production can be calculated by converting the cost of electricity and water consumption. The cost of electricity can take into account surplus power generated from wind, solar, and hydropower, which can significantly reduce the cost of hydrogen production. At the same time, the energy consumed per unit of time to produce one mole of hydrogen is defined as the energy consumption ratio [33], which is expressed as follows:

$$C_E = \frac{U_{cell} \times I_{cell} + \frac{\left(F^{an}_{H_2O,out} + F_{H_2O,con} + F^{cat}_{H_2O,out}\right) \times \frac{18 \times g \times h_w}{1000}}{0.85}}{F_{H_2,gen}} \tag{17}$$

The specific variable in the formula is shown in Table 17.

Table 17. Variable of the energy consumption ratio formula.

	Symbol	Name	Unit
Variable	C_E	Energy consumption ratio	J/mol/s

4.4. PEM Electrolysis Device's Self-Sustaining Control Interval Division

In the PEM electrolysis device, the optimal operating temperature of the cathode and anode is 338.15 K, and the division for the self-sustaining control interval is specified as follows:

(1) When the operating temperature of the cathode or anode is in the range of 323.15–353.15 K, the disturbance observation method is adopted to adjust the molar flow rate of the cathode or anode water outlet, so that the operating temperature keeps tracking the optimum value of 338.15 K by changing the heat lost internally.

(2) When the operating temperature of the cathode or anode is lower than 323.15 K, the gradient-rise method is used to reduce the molar flow rate of the cathode or anode water outlet, so that the operating temperature quickly returns to the normal operating temperature by changing the heat lost internally.

(3) When the operating temperature of the cathode or anode is greater than 353.15 K, the gradient-down method is used to reduce the operating voltage, so that the operating temperature can be quickly restored to the normal operating temperature by changing the generated heat internally.

In summary, and based on the electrothermal-coupling dynamic model of the PEM electrolysis device, the operating voltage and the molar flow rates of water outlet of the cathode and anode are used as the control variables; the molar flow rates of gas outlet of the cathode and anode are used as the disturbance variables; and the operating temperature of the cathode and anode are used as state variables. The gradient-disturbance observation method is used according to the division of operating temperature to make the operating temperature of the cathode and the anode constant under the variation of input power at near the set value of 338.15 K in order to improve the hydrogen production rate and electrolysis efficiency. The details are shown in Figure 6.

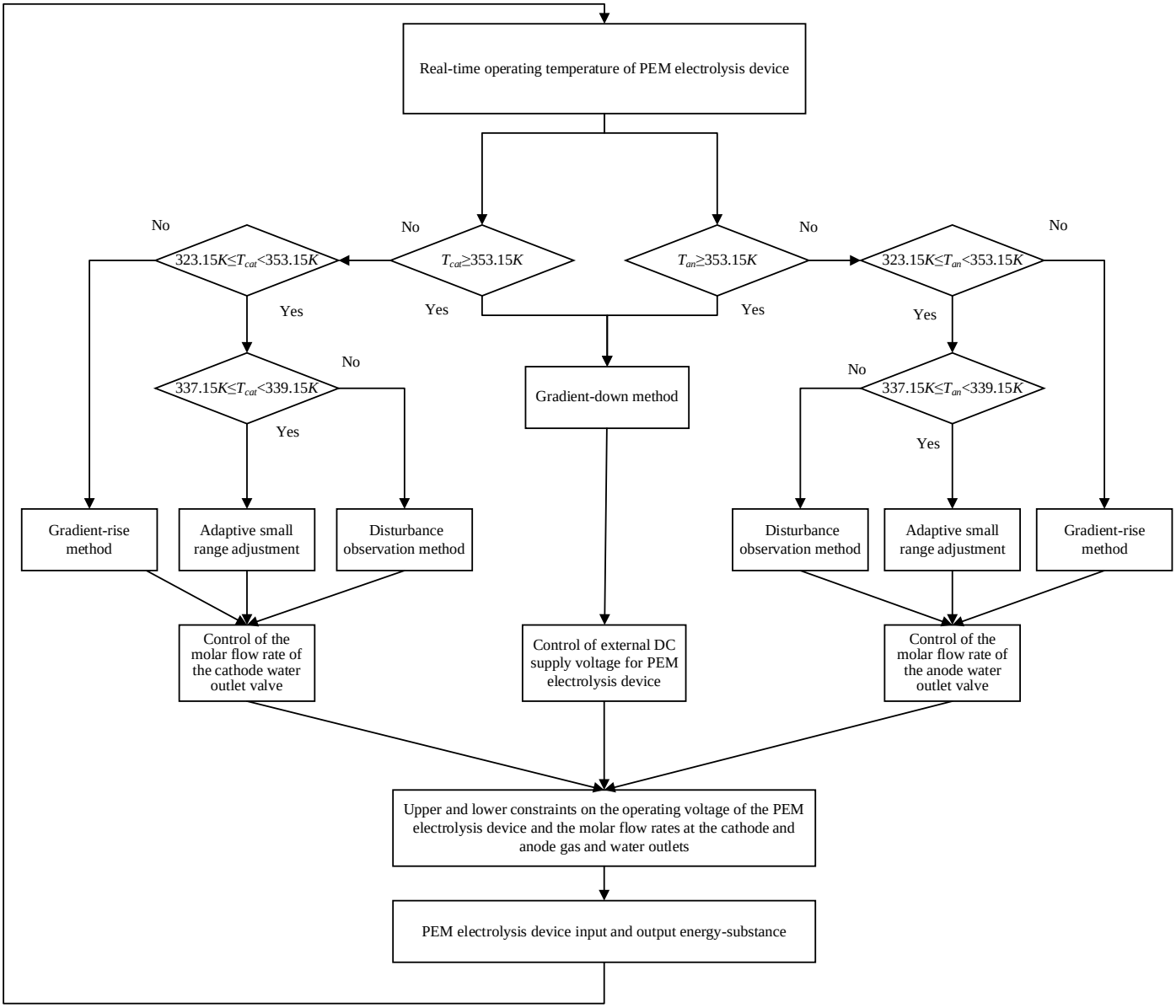

Figure 6. Flow chart of the self-sustaining control strategy.

The upper and lower bound constraints on the molar flow rates at the cathode and anode gas and water outlets are specified as follows:

$$\begin{cases} F_{H_2,out} = F_{H_2,gen} \\ F_{H_2O,mem} \le F_{H_2O,out}^{cat} \le 0.14\ \text{mol/s} \\ F_{O_2,out} = F_{O_2,gen} \\ 0 \le F_{H_2O,out}^{an} \le 0.14\ \text{mol/s} \end{cases} \tag{18}$$

The direction that causes the fastest change in operating temperature is along the gradient direction of the relationship function between the operating temperature and the cathode and anode water export molar flow rates and operating voltage; this can be performed by adjusting the cathode and anode water export molar flow rates and the operating voltage, followed by adjusting the operating temperature, as determined by the following formula:

$$\begin{cases} \frac{\partial T_{cat}}{\partial U_{cell}} = \frac{\frac{1}{2}\times I_{cell}}{0.5C_t} & \frac{\partial T_{an}}{\partial U_{cell}} = \frac{\frac{1}{2}\times I_{cell}}{0.5C_t} \\ \frac{\partial T_{cat}}{\partial F_{H_2O,out}^{cat}} = \frac{C_{H_2O,v,m}\times(T_{cat}-T_1)}{0.5C_t} & \frac{\partial T_{an}}{\partial F_{H_2O,out}^{an}} = \frac{C_{H_2O,v,m}\times(T_{an}-T_1)}{0.5C_t} \end{cases} \tag{19}$$

The learning rate of the gradient method is the step size of the control variable update. The dynamic equivalent circuit of the PEM electrolysis device is a first-order circuit; when the excitation changes abruptly, the response changes dynamically at $1/\tau$ rate, and when τ_{cat} is maximum, then the learning rate is set as follows:

$$\alpha = 0.000001\frac{1}{\tau_{cat}} \tag{20}$$

The specific variable in the formula is shown in Table 18.

Table 18. Variable of the gradient method learning rate formula.

	Symbol	Name	Unit
Variable	α	Learning rate of gradient method	-

In the range of $T_1 \le T_{cat} < 323.15$ K or $T_1 \le T_{an} < 323.15$ K, a gradient-rise method is used to increase the operating temperature by reducing the molar flow rate of the water outlet in the cathode or the anode as follows:

$$\begin{cases} F_{H_2O,out}^{cat} = F_{H_2O,out}^{cat,new} = F_{H_2O,out}^{cat,old} - \alpha \times \frac{\partial T_{cat}}{\partial F_{H_2O,out}^{cat}} \\ F_{H_2O,out}^{an} = F_{H_2O,out}^{an,new} = F_{H_2O,out}^{an,old} - \alpha \times \frac{\partial T_{an}}{\partial F_{H_2O,out}^{an}} \end{cases} \tag{21}$$

The specific variables in the formula are shown in Table 19.

Table 19. Variables of the gradient-rise method formula.

	Symbol	Name	Unit
Variables	$F_{H_2O,out}^{cat,new}$	New value after updating the molar flow rate of the water outlet in the cathode	mol/s
	$F_{H_2O,out}^{cat,old}$	Old value before updating the molar flow rate of the water outlet in the cathode	mol/s
	$F_{H_2O,out}^{an,new}$	New value after updating the molar flow rate of the water outlet in the anode	mol/s
	$F_{H_2O,out}^{an,old}$	Old value before updating the molar flow rate of the water outlet in the anode	mol/s

In the range of 323.15 K $\leq T_{cat}$ < 353.15 K or 323.15 K $\leq T_{an}$ < 353.15 K, to make the cathode or the anode operate near the optimal operating temperature of 338.15 K, the operating temperature interval is divided by T_{cat} = 338.15 K or T_{an} = 338.15 K, and the disturbance observation method is used within the control variable's constraint. The current optimal value is continuously accepted to indirectly control T_{cat} and T_{an}, and the difference between the new value after disturbance and the old value before disturbance is specified as follows:

$$\begin{cases} \Delta F^{cat}_{H_2O,out} = F^{cat,new}_{H_2O,out} - F^{cat,old}_{H_2O,out} \\ \Delta F^{an}_{H_2O,out} = F^{an,new}_{H_2O,out} - F^{an,old}_{H_2O,out} \end{cases} \tag{22}$$

The specific variables in the formula are shown in Table 20.

Table 20. Variables of the formula for the disturbance observation method.

	Symbol	Name	Unit
Variables	$\Delta F^{cat}_{H_2O,out}$	Difference between the new value and the old value of the molar flow rate at the water outlet in the cathode after and before the update	mol/s
	$\Delta F^{an}_{H_2O,out}$	Difference between the new value and the old value of the molar flow rate at the water outlet in the anode after and before the update	mol/s

In the range of 323.15 K $\leq T_{cat}$ < 338.15 K or 323.15 K $\leq T_{an}$ < 338.15 K, the operating temperature is increased by reducing the molar flow rate of the water outlet in the cathode or the anode as follows:

$$\begin{cases} F^{cat}_{H_2O,out} = F^{cat,new}_{H_2O,out} & \Delta F^{cat}_{H_2O,out} \leq 0 \\ F^{an}_{H_2O,out} = F^{an,new}_{H_2O,out} & \Delta F^{an}_{H_2O,out} \leq 0 \end{cases} \tag{23}$$

In the range of 338.15 K $\leq T_{cat}$ < 353.15 K or 338.15 K $\leq T_{an}$ < 353.15 K, the operating temperature is reduced by increasing the molar flow rate of the water outlet in the cathode or the anode as follows:

$$\begin{cases} F^{cat}_{H_2O,out} = F^{cat,new}_{H_2O,out} & \Delta F^{cat}_{H_2O,out} > 0 \\ F^{an}_{H_2O,out} = F^{an,new}_{H_2O,out} & \Delta F^{an}_{H_2O,out} > 0 \end{cases} \tag{24}$$

To regulate the operating temperature of the cathode or the anode more smoothly, the operating voltage that changes with the input power is introduced when there is little fluctuation around T_{cat} = 338.15 K or T_{an} = 338.15 K, and small amplitude adaptive regulation is used as follows:

$$\begin{cases} F^{cat}_{H_2O,out} = F^{cat,new}_{H_2O,out} = F^{cat,old}_{H_2O,out} \mp 10^{-5} U_{cell} & (337.65 \mp 0.5)K < T_{cat} \leq (338.65 \mp 0.5)K \\ F^{an}_{H_2O,out} = F^{an,new}_{H_2O,out} = F^{an,old}_{H_2O,out} \mp 10^{-5} U_{cell} & (337.65 \mp 0.5)K < T_{an} \leq (338.65 \mp 0.5)K \end{cases} \tag{25}$$

In the range of $T_{cat} \geq$ 353.15 K or $T_{an} \geq$ 353.15 K, the molar flow rate of the water outlet in the cathode or the anode is increased at this time by using the disturbance observation method to reach the upper limit. To reduce the heat generated by the operating current and avoid high-temperature damage, a gradient-down method is used to adjust the operating voltage to reduce the operating current as follows:

$$U_{cell} = U^{new}_{cell} = U^{old}_{cell} - \alpha \times \left(\frac{\partial T_{cat}}{\partial U_{cell}} + \frac{\partial T_{an}}{\partial U_{cell}}\right) \tag{26}$$

The specific variables in the formula are shown in Table 21.

Table 21. Variables of the gradient-down method formula.

	Symbol	Name	Unit
Variables	U_{cell}^{new}	New value after operating voltage update	mol/s
	U_{cell}^{old}	Old value before operating voltage update	mol/s

5. Example Analysis

5.1. Rated Operating Conditions of the PEM Hydrogen Production System

For PEM water electrolysis devices, the values of αcat and αan are usually taken as 0.5 and 2 [34], respectively, while a is equal to 1 [19], as stated in the literature. In the present study, a single PEM electrolysis device has a rated power of 500 W and a proton-exchange membrane area of 160 cm^2, with the anode using Ir-based catalysts and the cathode using Pt-based catalysts. The corresponding $J_{0,cat}$ and $J_{0,an}$ values are 1×10^{-3} and 1×10^{-6} [28], respectively. In most of the literature, during the process of modeling PEM electrolysis devices or stacks, only a single electrolysis device is considered, and it is assumed that all single electrolysis devices in the stack have the same dynamic behavior [35]. Therefore, linear stack parameters are calculated based on the parameters of a single PEM electrolysis device and the number of linearly stacked PEM electrolysis devices. In this study, a simulation experimental analysis is performed by linearly stacking 100 PEM electrolysis devices to form a hydrogen production system. The rated power of the PEM hydrogen production system is 50,000 W, and the specific operating conditions are shown in Table 22.

Table 22. Parameters of the PEM hydrogen production system's rated operating conditions.

	Symbol	Name	Value	Unit
Parameters	P_{cell}	Rated power	50,000	W
	T_{an}	Anode operating temperature	338.15	K
	T_{cat}	Cathode operating temperature	338.15	K
	$F_{H_2O,out}^{an}$	Molar flow rate of the anode water outlet	1.4	mol/s
	$F_{H_2O,out}^{cat}$	Molar flow rate of the cathode water outlet	2	mol/s
	η_{cell}	Electrolysis efficiency	74.3%	-
	n_{cell}	Number of stacked PEM electrolysis devices	100	-
	A_{mem}	PEM area	160	cm^2
	a	Water activity in the anode	1	-
	α_{cat}	Typical values for the charge transfer coefficient at the cathode	0.25	-
	α_{an}	Typical values for the charge transfer coefficient at the anode	0.8	-
	$J_{0,cat}$	Exchange current density on the cathode electrode	10^{-3}	-
	$J_{0,an}$	Exchange current density on the anode electrode	10^{-6}	-

5.2. Comparative Analysis of Cathode and Anode Operating Temperatures

The same power is input to the PEM hydrogen production system under the uncontrolled mode and the self-sustaining controlled mode operation, and a variable input power comparison simulation experiment is conducted, where the input power is shown in Figure 7.

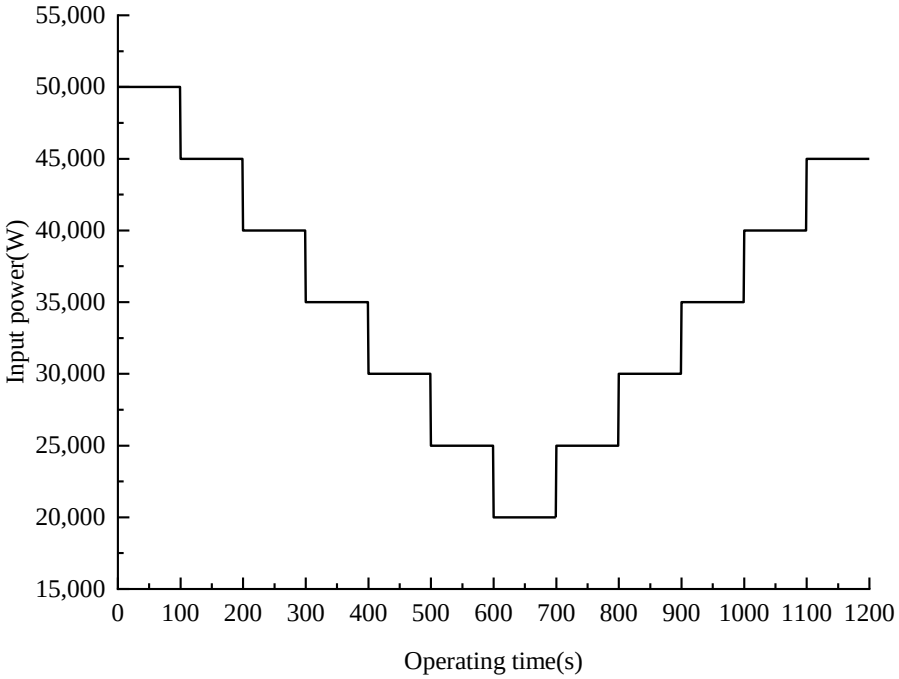

Figure 7. Input power of the PEM hydrogen production system.

From the start of the PEM hydrogen production system to the end of the input power change cycle, the self-sustaining controlled mode reaches the normal operating temperature earlier than the uncontrolled mode, and fluctuates around the optimal operating temperature of 338.15 K, as shown in Figures 8 and 9.

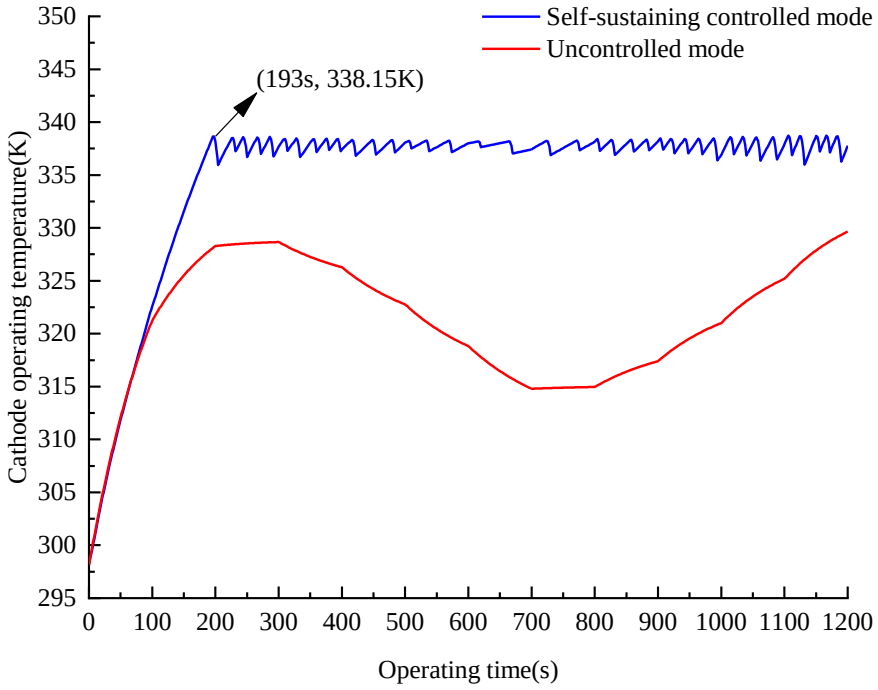

Figure 8. Cathode operating temperature.

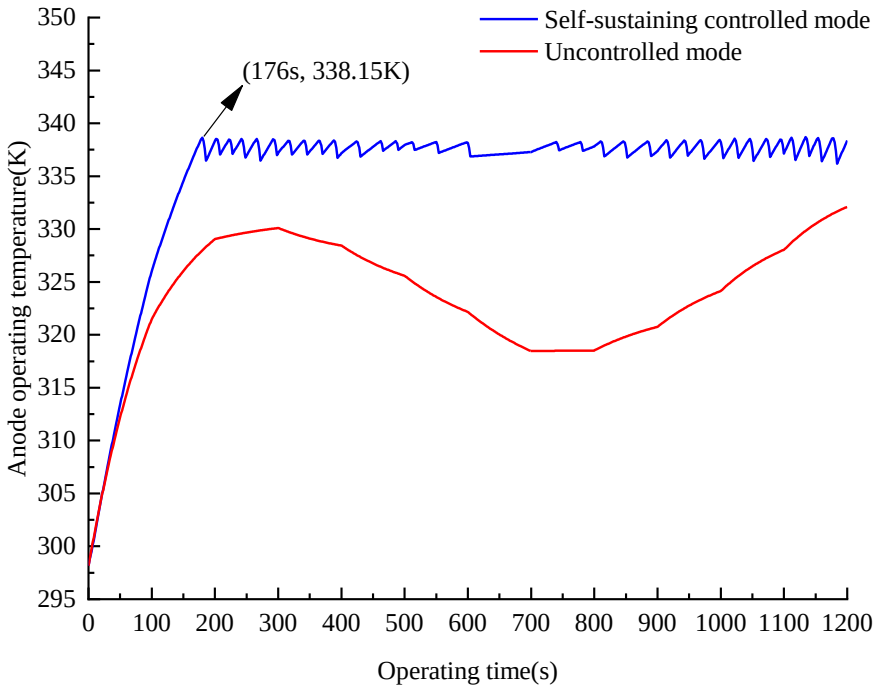

Figure 9. Anode operating temperature.

5.3. Comparative Analysis of Operating Voltage and Current

From the start of the PEM hydrogen production system to the end of the input power change cycle, due to the temperature being maintained near the optimum value under the self-sustaining controlled mode, the electrochemical reaction rate is accelerated. Compared to the uncontrolled mode, the operating voltage is lower and the operating current is higher, as shown in Figures 10 and 11.

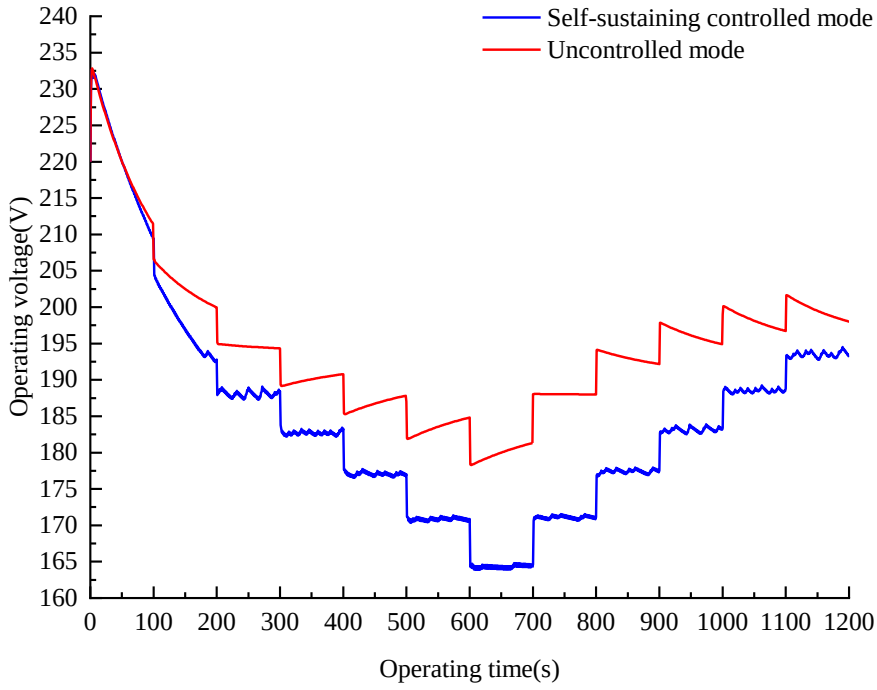

Figure 10. Operating voltage.

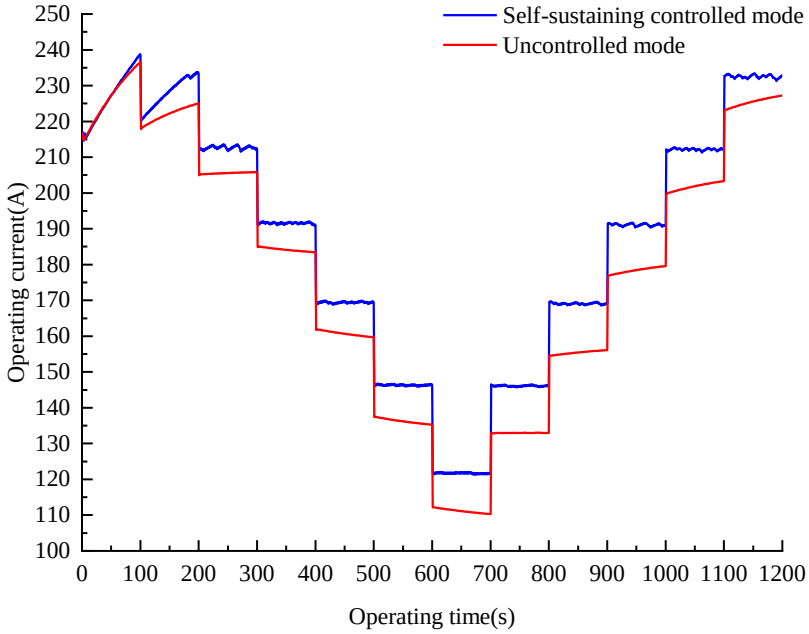

Figure 11. Operating current.

5.4. Comparative Analysis of Hydrogen and Oxygen Production Rates and Production Volumes, as well as Cathode and Anode Water Intake

From the start of the PEM hydrogen production system to the end of the input power change period, due to the self-sustaining controlled mode having a higher operating current than the uncontrolled mode, according to Faraday's law, the average hydrogen and oxygen production rates are increased by 0.275 mol/min and 0.14 mol/min, respectively, while the hydrogen and oxygen production volumes are increased by 5.5 mol and 2.8 mol, respectively. The water intakes of the anode and cathode are reduced by 1064.3 mol and 1231.8 mol, respectively. The input energy–substance decreases while the output energy–substance increases, as shown in Figures 12–17.

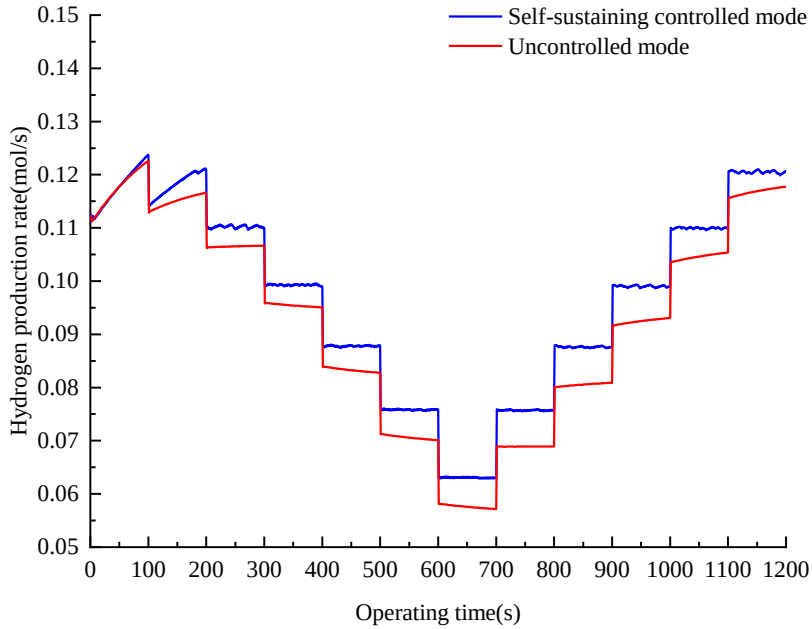

Figure 12. Hydrogen production rate.

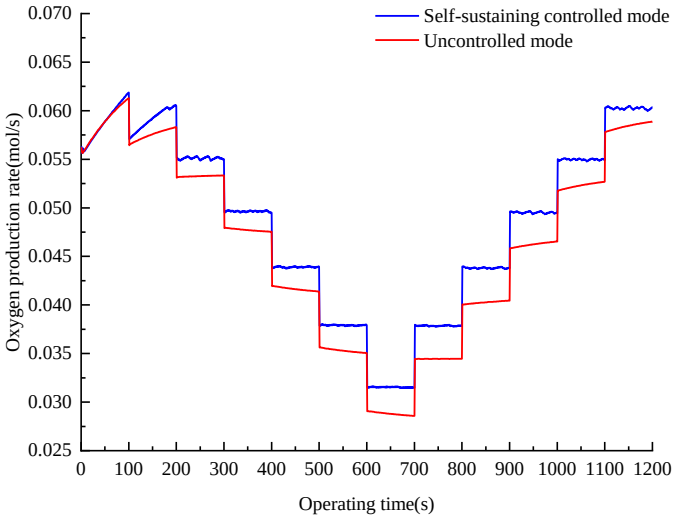

Figure 13. Oxygen production rate.

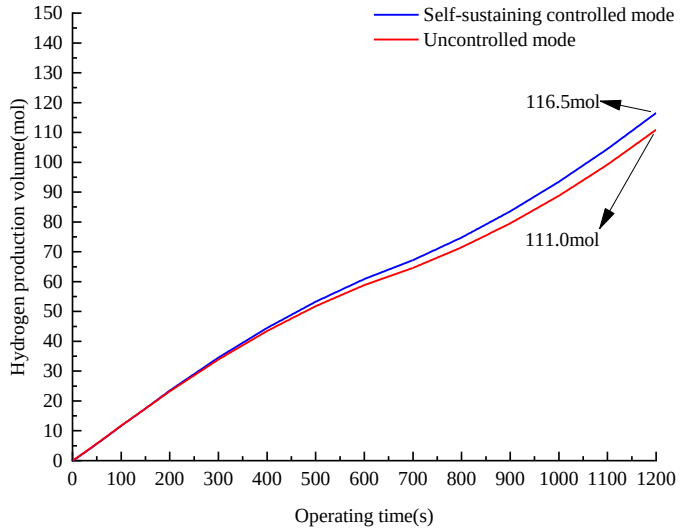

Figure 14. Hydrogen production volume.

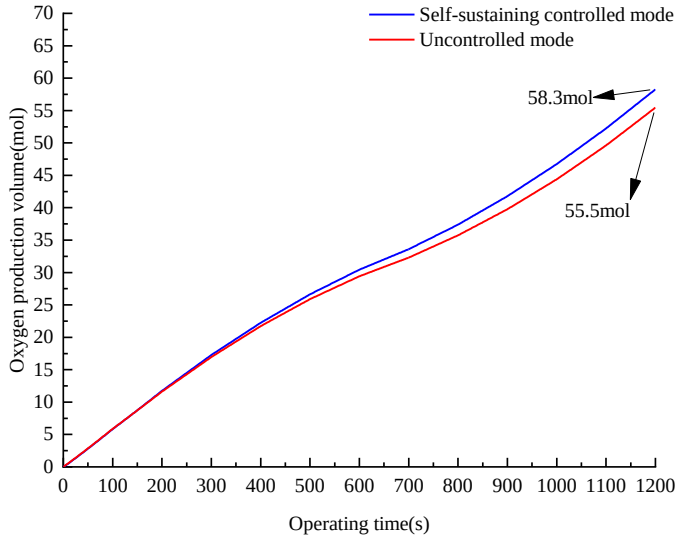

Figure 15. Oxygen production volume.

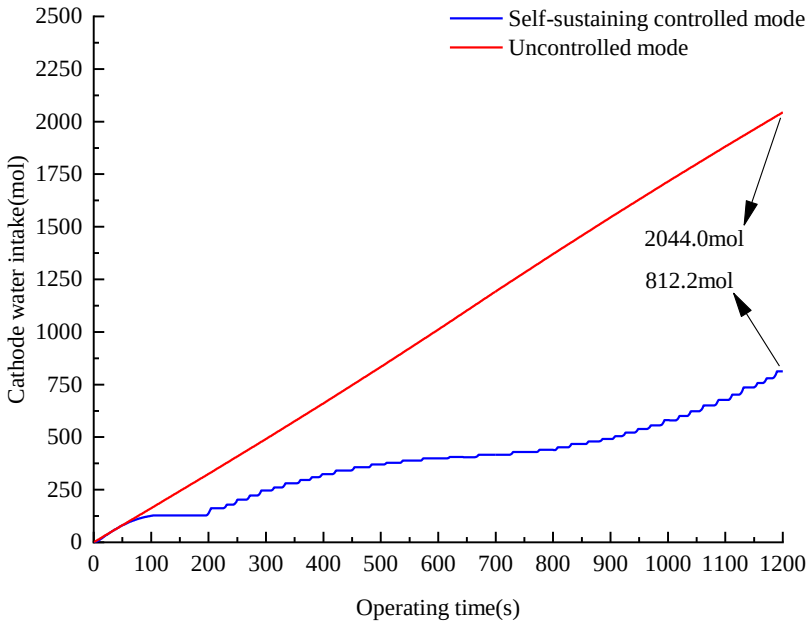

Figure 16. Cathode water intake.

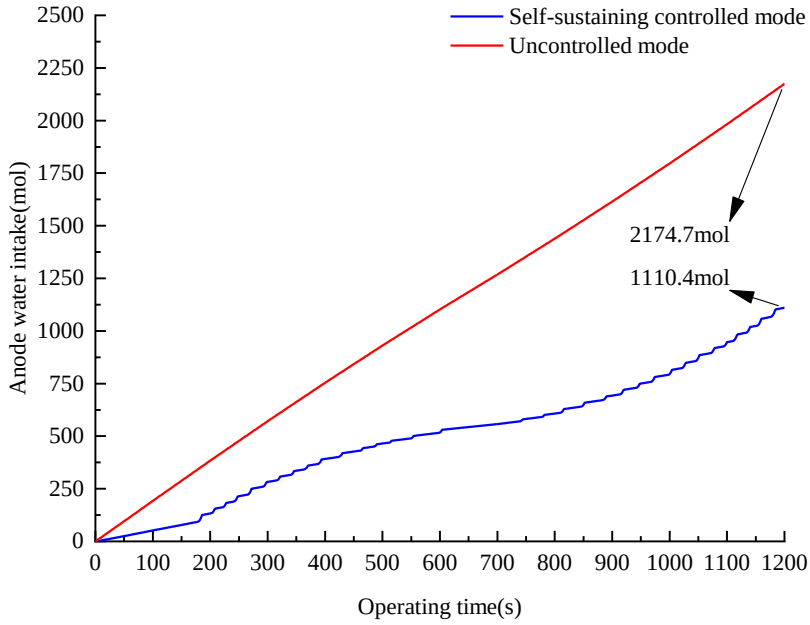

Figure 17. Anode water intake.

5.5. Comparative Analysis of Electrolysis Efficiency and Energy Consumption Ratio

From the start of the PEM hydrogen production system to the end of the input power change period, the self-sustaining controlled mode has a higher electrolysis efficiency and lower energy consumption ratio than the uncontrolled mode, with an increase in electrolysis efficiency of 3.9%, as shown in Figures 18 and 19.

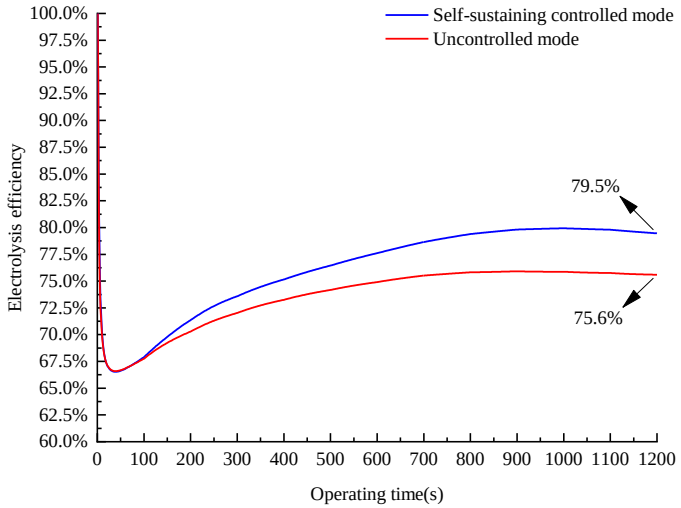

Figure 18. Electrolysis efficiency.

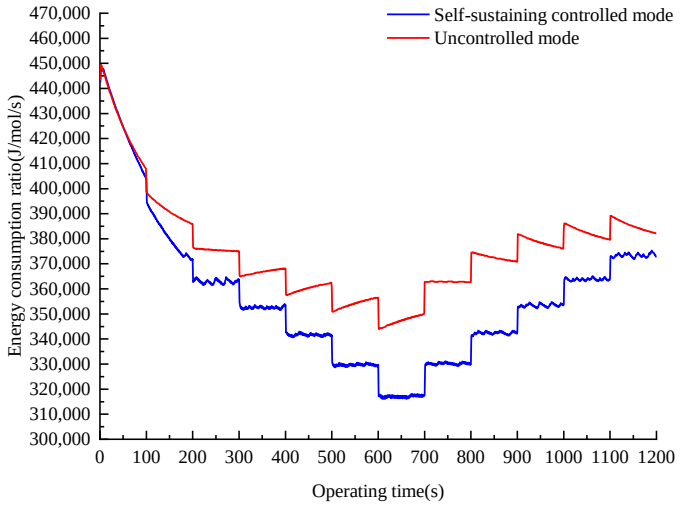

Figure 19. Energy consumption ratio.

6. Conclusions

Based on the energy–substance conservation principle of PEM electrolysis devices and by taking into account various factors, such as temperature and current, during the operation process, an electrothermal-coupling dynamic model was constructed. A self-sustaining control strategy based on the gradient-disturbance observation method is designed. Without the need for an external cooling device, the temperature of the anode and cathode can be dynamically adjusted using the heat generated and lost during the operation to maintain a high hydrogen production rate and high electrolysis efficiency.

A simulation model of a hydrogen production system with 100 linearly stacked PEM electrolysis devices was built in the MATLAB/Simulink environment. A comparative analysis of the operating temperature, operating voltage, operating current, inlet flow rate, hydrogen and oxygen production volumes, hydrogen production rate, oxygen production rate, electrolysis efficiency, and energy consumption ratio was carried out between the self-sustaining controlled mode and the uncontrolled mode. The following conclusions are obtained:

(1) The electrothermal-coupling dynamic model of PEM electrolysis devices fully considers factors such as heat carried away by hydrogen and oxygen and difference in temperature between the anode and cathode, which is more in line with the actual situation.

(2) By considering the efficiency and the work performed by the water circulation device, the PEM hydrogen production system itself and the external water circulation device are regarded as a whole energy–substance system, and a new concept of electrolysis efficiency is defined, which fully reflects the energy–substance conversion of the entire process of electrolyzing water to produce hydrogen.
(3) The PEM hydrogen production system can maintain the operating temperature of the anode and cathode at around 338.15 K even if the input power changes in the self-sustaining controlled mode.
(4) The operating voltage of the PEM hydrogen production system in the self-sustaining controlled mode is lower and the operating current is higher than those in the uncontrolled mode.
(5) In the self-sustaining controlled mode, the PEM hydrogen production system lowers the water intake by 1064.3 mol and 1231.8 mol for the anode and the cathode, respectively, and the average hydrogen and oxygen production rates are increased by 0.275 mol/min and 0.14 mol/min, respectively. The hydrogen and oxygen production volumes are increased by 5.5 mol and 2.8 mol, respectively, while requiring less water.
(6) In the self-sustaining controlled mode, the electrolysis efficiency of the PEM hydrogen production system is improved by 3.9% compared to the uncontrolled mode, and it has a lower energy consumption ratio.

Author Contributions: Conceptualization and methodology, Z.G. and Y.T.; simulation and analysis, Z.G.; investigation, Y.T.; data curation, Z.G.; writing—original draft preparation, Z.G.; writing—review and editing, Z.G. and Y.T.; supervision, Y.T.; literature research, Z.G. All authors have read and agreed to the published version of the manuscript.

Funding: This research was funded by the Key R & D Projects of Xinjiang Uygur Autonomous Region, grant number 2022B01016 and the Natural Science Foundation of Xinjiang Uygur Autonomous Region, grant number 2022D01C364.

Data Availability Statement: Not applicable.

Conflicts of Interest: The authors declare no conflict of interest.

References

1. Aubras, F.; Deseure, J.; Kadjo, J.-J.; Dedigama, I.; Majasan, J.; Grondin-Perez, B.; Chabriat, J.-P.; Brett, D. Two-dimensional model of low-pressure PEM electrolyser: Two-phase flow regime, electrochemical modelling and experimental validation. *Int. J. Hydrogen Energy* **2017**, *42*, 26203–26216. [CrossRef]
2. Feng, Q.; Yuan, Z.; Liu, G.; Wei, B.; Zhang, Z.; Li, H.; Wang, H. A review of proton exchange membrane water electrolysis on degradation mechanisms and mitigation strategies. *J. Power Sources* **2017**, *366*, 33–55. [CrossRef]
3. Tijani, A.S.; Ghani, M.A.; Rahim, A.H.A.; Muritala, I.K.; Mazlan, F.A.B. Electrochemical characteristics of (PEM) electrolyzer under influence of charge transfer coefficient. *Int. J. Hydrogen Energy* **2019**, *44*, 27177–27189. [CrossRef]
4. Kumar, S.S.; Himabindu, V. Hydrogen production by PEM water electrolysis—A review. *Mater. Sci. Energy Technol.* **2019**, *2*, 442–454. [CrossRef]
5. Dale, N.; Mann, M.; Salehfar, H. Semiempirical model based on thermodynamic principles for determining 6kW proton exchange membrane electrolyzer stack characteristics. *J. Power Sources* **2008**, *185*, 1348–1353. [CrossRef]
6. Uchman, W.; Kotowicz, J. Varying load distribution impacts on the operation of a hydrogen generator plant. *Int. J. Hydrogen Energy* **2021**, *46*, 39095–39107. [CrossRef]
7. Nasser, M.; Hassan, H. Techno-enviro-economic analysis of hydrogen production via low and high temperature electrolyzers powered by PV/Wind turbines/Waste heat. *Energy Convers. Manag.* **2023**, *278*, 116693. [CrossRef]
8. Li, J. *Study on Influencing Factors of Hydrogen Production by Electrolyzing Water*; Beijing University of Civil Engineering and Architecture: Beijing, China, 2020.
9. Hammoudi, M.; Henao, C.; Agbossou, K.; Dubé, Y.; Doumbia, M. New multi-physics approach for modelling and design of alkaline electrolyzers. *Int. J. Hydrogen Energy* **2012**, *37*, 13895–13913. [CrossRef]
10. Correa, G.; Marocco, P.; Muñoz, P.; Falagüerra, T.; Ferrero, D.; Santarelli, M. Pressurized PEM water electrolysis: Dynamic modelling focusing on the cathode side. *Int. J. Hydrogen Energy* **2021**, *47*, 4315–4327. [CrossRef]
11. Dang, J.; Yang, F.; Li, Y.; Zhao, Y.; Ouyang, M.; Hu, S. Experiments and microsimulation of high-pressure single-cell PEM electrolyzer. *Appl. Energy* **2022**, *321*, 119351. [CrossRef]

12. Guilbert, D.; Vitale, G. Dynamic Emulation of a PEM Electrolyzer by Time Constant Based Exponential Model. *Energies* **2019**, *12*, 750. [CrossRef]
13. García-Valverde, R.; Espinosa, N.; Urbina, A. Simple PEM water electrolyser model and experimental validation. *Int. J. Hydrogen Energy* **2012**, *37*, 1927–1938. [CrossRef]
14. García-Valverde, R.; Miguel, C.; Martínez-Béjar, R.; Urbina, A. Optimized photovoltaic generator–water electrolyser coupling through a controlled DC–DC converter. *Int. J. Hydrog. Energy* **2008**, *33*, 5352–5362. [CrossRef]
15. Rauls, E.; Hehemann, M.; Keller, R.; Scheepers, F.; Müller, M.; Stolten, D. Favorable Start-Up behavior of polymer electrolyte membrane water electrolyzers. *Appl. Energy* **2023**, *330*, 120350. [CrossRef]
16. Cilogluları, M.; Erden, M.; Karakilcik, M.; Dincer, I. Investigation of hydrogen production performance of a Photovoltaic and Thermal System. *Int. J. Hydrogen Energy* **2016**, *42*, 2547–2552. [CrossRef]
17. Ali, D.; Gazey, R.; Aklil, D. Developing a thermally compensated electrolyser model coupled with pressurised hy-drogen storage for modelling the energy efficiency of hydrogen energy storage systems and identifying their operation per-formance issues. *Renew. Sust. Energ. Rev.* **2016**, *66*, 27–37. [CrossRef]
18. Chandesris, M.; Médeau, V.; Guillet, N.; Chelghoum, S.; Thoby, D.; Fouda-Onana, F. Membrane degradation in PEM water electrolyzer: Numerical modeling and experimental evidence of the influence of temperature and current density. *Int. J. Hydrogen Energy* **2015**, *40*, 1353–1366. [CrossRef]
19. Wang, Z.; Wang, X.; Chen, Z.; Liao, Z.; Xu, C.; Du, X. Energy and exergy analysis of a proton exchange membrane water electrolysis system without additional internal cooling. *Renew. Energy* **2021**, *180*, 1333–1343. [CrossRef]
20. Liu, X.; Yin, Y.; Li, M.; Yang, C.; Li, T. Development and test of a low cost new PEM water electrolyzer. *Space Med. Med. Eng.* **2020**, *33*, 350–355.
21. Atlam, O.; Kolhe, M. Equivalent electrical model for a proton exchange membrane (PEM) electrolyser. *Energy Convers. Manag.* **2011**, *52*, 2952–2957. [CrossRef]
22. Keddar, M.; Zhang, Z.; Periasamy, C.; Doumbia, M.L. Power quality improvement for 20 MW PEM water electrolysis system. *Int. J. Hydrog. Energy* **2022**, *47*, 40184–40195. [CrossRef]
23. Tjarks, G.; Gibelhaus, A.; Lanzerath, F.; Müller, M.; Bardow, A.; Stolten, D. Energetically-optimal PEM electrolyzer pressure in power-to-gas plants. *Appl. Energy* **2018**, *218*, 192–198. [CrossRef]
24. Guilbert, D.; Vitale, G. Experimental Validation of an Equivalent Dynamic Electrical Model for a Proton Exchange Mem-brane Electrolyzer. In Proceedings of the 2018 IEEE International Conference on Environment and Electrical Engineering and 2018 IEEE Industrial and Commercial Power Systems Europe (EEEIC/I&CPS Europe), Palermo, Italy, 12–15 June 2018; pp. 1–6.
25. Hernández-Gómez, Á.; Ramirez, V.; Guilbert, D.; Saldivar, B. Development of an adaptive static-dynamic electrical model based on input electrical energy for PEM water electrolysis. *Int. J. Hydrogen Energy* **2020**, *45*, 18817–18830. [CrossRef]
26. Hernández-Gómez, Á.; Ramirez, V.; Guilbert, D.; Saldivar, B. Cell voltage static-dynamic modeling of a PEM electrolyzer based on adaptive parameters: Development and experimental validation. *Renew. Energy* **2021**, *163*, 1508–1522. [CrossRef]
27. Lebbal, M.; Lecœuche, S. Identification and monitoring of a PEM electrolyser based on dynamical modelling. *Int. J. Hydrog. Energy* **2009**, *34*, 5992–5999. [CrossRef]
28. Han, B.; Steen, S.M.; Mo, J.; Zhang, F.-Y. Electrochemical performance modeling of a proton exchange mem-brane electrolyzer cell for hydrogen energy. *Int. J. Hydrog. Energy* **2015**, *40*, 7006–7016. [CrossRef]
29. da Costa Lopes, F.; Watanabe, E.H. Experimental and theoretical development of a PEM electrolyzer model applied to energy storage systems. In Proceedings of the 2009 Brazilian Power Electronics Conference, Bonito-Mato Grosso do Sul, Brazil, 27 September–1 October 2009; pp. 775–782.
30. Nafchi, F.M.; Afshari, E.; Baniasadi, E.; Javani, N. A parametric study of polymer membrane electrolyser performance, energy and exergy analyses. *Int. J. Hydrog. Energy* **2018**, *44*, 18662–18670. [CrossRef]
31. Yodwong, B.; Guilbert, D.; Phattanasak, M.; Kaewmanee, W.; Hinaje, M.; Vitale, G. Faraday's Efficiency Modeling of a Proton Exchange Membrane Electrolyzer Based on Experimental Data. *Energies* **2020**, *13*, 4792. [CrossRef]
32. Yiğit, T.; Selamet, O.F. Mathematical modeling and dynamic Simulink simulation of high-pressure PEM electrolyzer system. *Int. J. Hydrog. Energy* **2016**, *41*, 13901–13914. [CrossRef]
33. Ursua, A.; Gandia, L.M.; Sanchis, P. Hydrogen Production from Water Electrolysis: Current Status and Future Trends. *Proc. IEEE* **2012**, *100*, 410–426. [CrossRef]
34. Marangio, F.; Santarelli, M.; Calì, M. Theoretical model and experimental analysis of a high pressure PEM water electrolyser for hydrogen production. *Int. J. Hydrog. Energy* **2009**, *34*, 1143–1158. [CrossRef]
35. Olivier, P.; Bourasseau, C.; Bouamama, P.B. Low-temperature electrolysis system modelling: A review. *Renew. Sustain. Energy Rev.* **2017**, *78*, 280–300. [CrossRef]